CFD Simulation of 1.5 MW HAWT with Vortex Generator

Ramesh Chinnappan, Mohanraj Chandran, G. Hari Prasanth, S. Navaneethan, and M. Harshankumar

Abstract Over the years, many developments have been encountered in both offshore and onshore wind turbine blade design. In this study, the aerodynamic effect of vortex generators in WindPACT 1.5 MW wind turbine blade is made by NREL. The turbine contains three types of airfoils, i.e., S818+, S825+, and S826+ which are developed by NREL. Vortex generator (VG) is attached with the wind turbine along throughout length of blade. Geometry was created in solid works software and meshed using a fluent watertight meshing workflow for better accuracy, the full-scale wind turbine CFD (computational fluid dynamics) analysis was done with ANSYS fluent solver, and series of computation was done to validate. The flow in the wind turbine with and without vortex indicator has been visualized. The aerodynamic structural effects and pressure distribution along the surface of the blade and their impact on the strength of the blade were studied. The results indicate that the vortex generators along the length of the blade reduce the flow separation over the blade surface and also maintain the pressure difference that causes the deformation of the blade.

Keywords Vortex generator · Flow separation · CFD

Abbreviations

CFD	Computational Fluid dynamics
HAWT	Horizontal axis wind turbine
NREL	National Renewable energy laboratory
SEM	Scanning Electron Microscope
VG	Vortex Generator

R. Chinnappan (✉) · M. Chandran · G. Hari Prasanth · S. Navaneethan · M. Harshankumar
Department of Mechanical Engineering, M.Kumarasamy College of Engineering, Karur, Tamilnadu 639113, India
e-mail: mkcecramesh@gmail.com

V. Edwin Geo and F. Aloui (eds.), *Energy and Exergy for Sustainable and Clean Environment, Volume 2*, Green Energy and Technology,
https://doi.org/10.1007/978-981-16-8274-2_26

1 Introduction

Life without energy has become unimaginable in this digital era. At the same time, the depletion of the non-renewable resources is increasing now and then. Hence, it is too urge to shift toward renewable resources. Wind is the alternate source of energy that produces the electricity from renewable wind power. The wind energy can be harvested in both the onshore and offshore regions. The onshore wind turbines are less expensive and are more efficient when compared to the offshore turbines, because the offshore turbine requires more landscapes for the installation. The wind energy in India began even from 1952. Since it is much essential to improve the efficiency of wind power, the NREL has been working with this and has made different models of airfoil shapes. Thus, we have utilized these shapes and analyzed by implementing the vortex generator into those models. The vortex generators are incorporated into each model along the length of the turbine blades with the help of solid works software and have done meshing in the ANSYS fluent software. Computational fluid dynamic analysis has been done for investigating the flow through the turbine in both the cases of with vortex generators and without vortex generators. We have analyzed the pressure, and the velocity impacts the turbine structure for the deformation. The NREL S809 aerofoil was analyzed, and it has been identified that the torque and thrust increase with the vortex generators. The vortex generator is capable of reducing the drag co-efficient at the certain particular angle of attacks, and they have also found that at the higher angle of attacks the lift co-efficients are further improved. Their work also revealed that the double vortex generators are capable of further reducing the thickness of the airfoils. Finally, the overall experiment revealed to us, in the airfoil S809, the better performance in the control of the flow separation along with the boundary layer offered by the double vortex generator [1]. The wind turbine aeroelastic analysis was carried out in the basic areas and cutting edge trends. They have identified that in the handling of the realistic models it is mandatory to model the system with various requirements such as wind shear and in the inflow of the wind at the complex areas, offshore applications with the hydrodynamic effects, the methods of manufacturing and the distribution of the materials, larger deflection which lead to the nonlinearity. The multidisciplinary framework system will be much useful to identify the configurations of the system and various possible control, structural, and various aerodynamic characteristics [2]. A thick wind turbine airfoil was analyzed with the application of vortex generators and validated the turbine sensitivity. The study reveals that with the increasing angle of attacks it reported that performance was improved with vortex generator. For the prediction of the aerodynamic performances, it is demonstrated that it is a step ahead to use the scale resolving simulations with respect to the promising tool and the RANS [3].

The wind turbine airfoil analyzed undergoing pitch oscillations and unsteady aerodynamics, and it is concluded that utilization of the passive vortex generators on the blades are highly promising. It was also identified that to more careful assess the performance characteristics of the vane height and the position along chordwise to get the overall better design of the air flows both in the case of the steady and the unsteady flows [4]. The composite structured wind turbine blade model was analyzed in multiple failure modes using general FEA modeling and found to be structure of blade influences more in failure of blades [5]. The impact of vortex generator on wind turbine blade profile was investigated and reported the installed VG upon the surface of the vortex generators where the expanding and contracting flow passages occur periodically. And the surface pressure at the reduced angles of attack is being changed only locally by the vortex generators but at the large angles of attack the vortex generators change the surface pressure along the entire airfoil [5]. The experimental investigation on the clay composite for wind turbine blades was carried out. And, it was identified that the optimum hardness and the higher tensile stress are obtained with the 1% montmorillonite composite and it is much suitable for the turbine blade applications. It has been made evident through the SEM and ANSYS analysis through images [6]. The material degradation in the composite turbine blades is analyzed for reliability, and it revealed that the reliability and the structural strength of the structure of the blade can be improved by using the composite materials. The sensitivity tests done in this work have revealed that the reliability of the blades should be identified only based upon the influence of the time [4]. Among those investigations, no work is found in the analysis of incorporating the vortex generator with NREL S818+, S825+, and S826 blade profiles.

The objective of this work is to analyze the effect of addition of vortex generator throughout the blade span in order to determine the intensity of flow separation, pressure and velocity distribution around the blade profiles by using the Ansys Fluent software. The results from inclusion vortex generator, such as flow profiles, pressure, and velocity distribution, were compared with the blade without vortex generator.

2 Materials and Methods

After comparing various wind turbine large scales, the NREL wind pact 1.5 MW wind turbine blade is selected for this study. The blade rotor is based on the 1.5 MW, and geometry was created based on reference Table 1. An old model three-bladed upwind HAWT with variable-speed variable pitch control. The details of the WindPACT 1.5 MW wind turbine are summarized in Table 1 and are referenced from WindPACT model Wind Turbines [7]. This blade has two shear webs and three types of airfoils, i.e., S818+, S825+, and S826+. The wind turbine blade 3D geometry was modeled using solid works and shown in Fig. 1. One-third wind turbine was modeled in order to decrease complexity and computational time.

Figure 1 shows the whole blade with airfoil placement along the span. According to Table 1, the blade is created three different airfoils. The hub is created using circular profile, and then, it is drafted to NREL S818 airfoil up to 16.15 m. Further, the NREL S825 airfoil is used to build the blade form 16.15 m to 29.45 m. Also, the blade tip was created by S826 airfoil. The lift and drag co-efficient changes of three airfoils based on different angle of attack are provided in Fig. 2. The S818 airfoil was set aerotwst angle about 11.1° which creates better lift and it was reduced gradually

Table 1 Wind turbine geometry definition

Distributed blade aerodynamic properties for the WindPACT 1.5-MW model				
Node (−)	RNodes (m)	AeroTwst (°)	Chord (m)	Airfoil (−)
1	2.85833	11.1	1.949	Circular Foil 0.5
2	5.075	11.1	2.269	s818
3	7.29167	11.1	2.589	s818
4	9.50833	10.41	2.743	s818
5	11.725	8.38	2.578	s818
6	13.94167	6.35	2.412	s818
7	16.15833	4.33	2.247	s818
8	18.375	2.85	2.082	s825
9	20.59167	2.22	1.916	s825
10	22.80833	1.58	1.751	s825
11	25.025	0.95	1.585	s825
12	27.24167	0.53	1.427	s825
13	29.45833	0.38	1.278	s825
14	31.675	0.23	1.129	s826
15	33.89167	0.08	0.98	s826

4.3°. Also, S825 was created and set from 2.85° to 0.38°. The tip was modeled 0.23° and 0.08°.

For considering the incompressible flow, the Navier stokes equation is simplified into

$$\frac{\partial p}{\partial t} + \frac{\partial}{\partial x_i}(\rho u_i) = 0 \tag{1}$$

$$\frac{\partial}{\partial t}(\rho u_i) + \frac{\partial}{\partial x_j}(\rho u_i u_j) = \frac{\partial}{\partial x_j}(\sigma_{ij}) - \frac{\partial p}{\partial x_i} - \frac{\partial \tau_{ij}}{\partial x_j} \tag{2}$$

The stress tensor is a function of viscosity and defined by

$$\sigma_{ij} \equiv \left[\mu\left(\frac{\partial u_i}{\partial x_j} + \frac{\partial u_j}{\partial x_i}\right)\right] - \frac{2}{3}\mu\frac{\partial u_l}{\partial x_l}\delta_{ij} \tag{3}$$

$$\tau_{ij} \equiv \rho u_i u_j(\text{avg}) - \rho u_i u_j(\text{ind}) \tag{4}$$

Using the Boussinesq technique, the sub-grid turbulent stresses are given as

$$\tau_{ij} - \frac{1}{3}\tau_{kk}\delta_{ij} = 2\mu_t S_{ij} \tag{5}$$

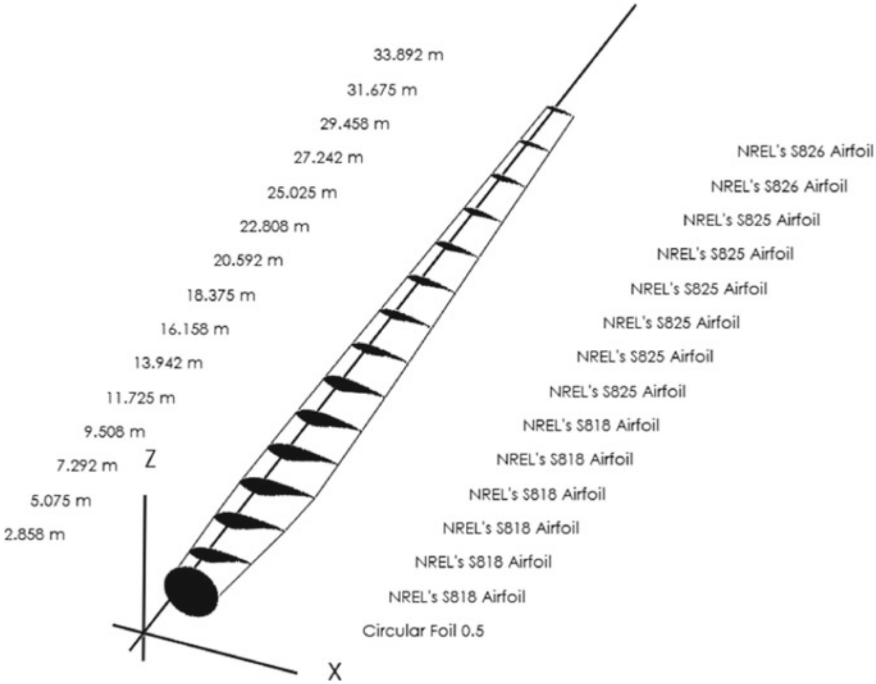

Fig. 1 Airfoil distribution along the span of blade

Here, μ_t turbulent viscosity in sub-grid scale.

The S_{ij} is a rate of strain tensor

$$S_{ij} \equiv \frac{1}{2}\left(\frac{\partial u_i}{\partial x_j} + \frac{\partial u_j}{\partial x_i}\right) \tag{6}$$

Among various sub-scale models such as smagorinsky-lilly, dynamic smagorinsky-lilly, WALE (wall adapting local eddy viscosity), and kinematic viscosity model, the turbulent kinematic energy and dissipation rate model was modeled to find accurate stresses.

Turbulence Kinetic Energy

$$\frac{\partial k}{\partial t} + U_j \frac{\partial k}{\partial x_j} = P_k - \beta^* k\omega + \frac{\partial}{\partial x_j}\left[(\nu + \sigma_k \nu_T)\frac{\partial k}{\partial x_j}\right] \tag{7}$$

Specific Dissipation Rate

$$\frac{\partial \omega}{\partial t} + U_j \frac{\partial \omega}{\partial x_j} = aS^2 - \beta\omega^2 \frac{\partial}{\partial x_j}\left[(\nu + \sigma_\omega \nu_T)\frac{\partial \omega}{\partial x_j}\right] + 2(1 - F_1)\sigma\omega^2 \frac{1}{\omega}\frac{\partial k}{\partial x_i}\frac{\partial \omega}{\partial x_j} \tag{8}$$

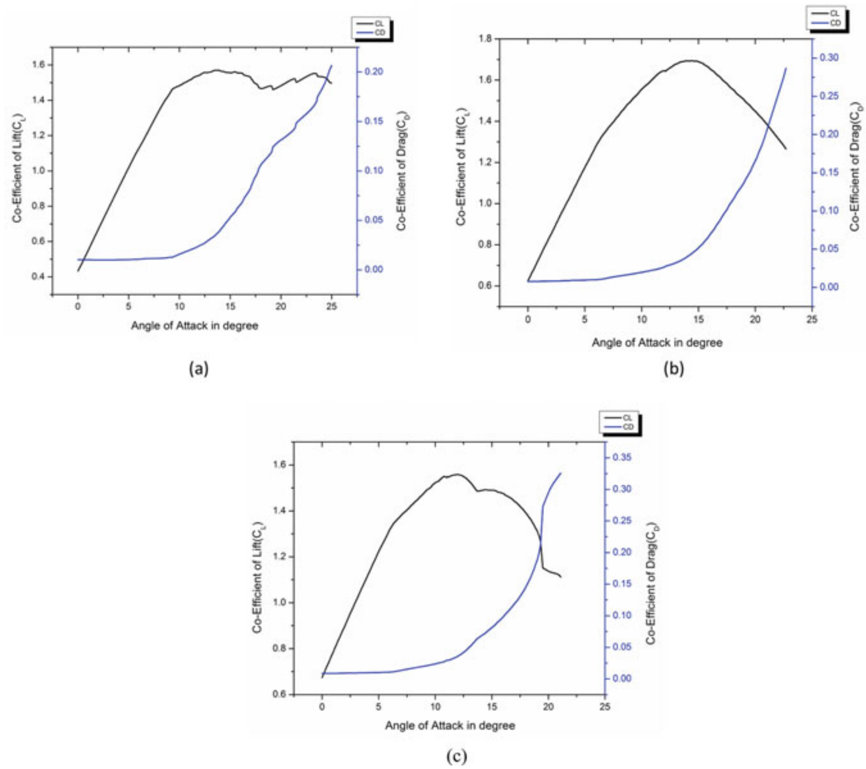

Fig. 2 Co-efficient of lift and drag Vs angle of attack: **a** S818, **b** S825, and **c** S826

Kinematic Eddy Viscosity

$$\nu_T = \frac{a_1 k}{\max(a_1 \omega, SF_2)} \tag{9}$$

2.1 Vortex Generator Configuration

Vortex generator configuration is designed and created based on Wang et al. [8] are shown in the following Equations:

The angle of the VG $(\beta) = 18°$.

The height of the VG $(Hvg) = \left(\frac{1}{100}\right) \times$ chordlength in m.

The length of the vortex generator $(Lvg) = 2 \times Hvg$ in m.

The distance between the trailing edges within a pair $(Svg) = 3 \times Hvg$ in m.

The distance between pairs $(Zvg) = 6 \times Hvg$ in m.

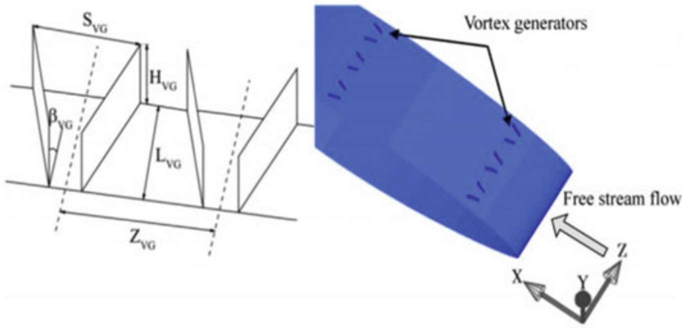

Fig. 3 Vortex generator configuration

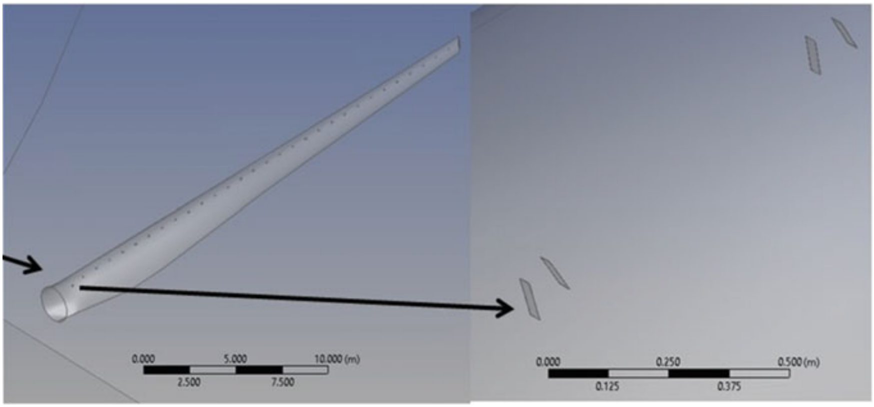

Fig. 4 Vortex generator placement along the blade length

Vortex generators are placed along the length of the Wind PACT blade. The horizontal length and vertical length of vortex generator are 27.43 mm and 54.86 mm, and angle from horizontal axis is 18°. Distance between two vanes is 82.29 mm, and distance between two vortex generator array configurations is 164.58 m (Figs. 3 and 4).

2.2 Mesh Generation and Boundary Conditions

The mesh for the wind turbine CFD analysis is generated using ANSYS watertight machine workflow for better accuracy in CFD analysis shown in Fig. 5. The Blade face sizing and inflation layers applied to have better resolution of boundary layer flow over the blade. Match control 120** rotation was applied for flow domain rotational periodicity. Mesh sensitivity study, i.e., +0.4 m, +0.2 m, +0.1 m, and +

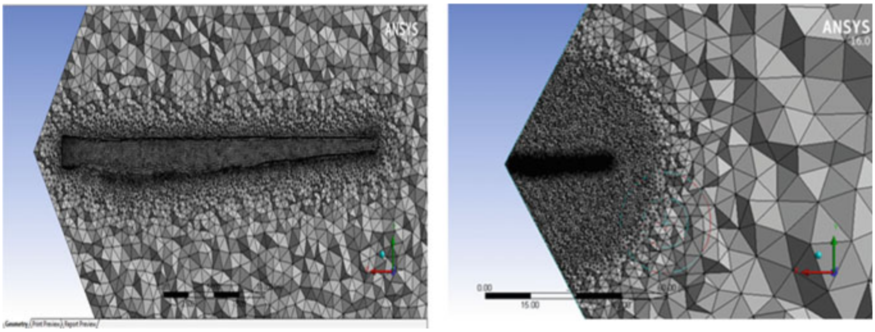

Fig. 5 Mesh generation

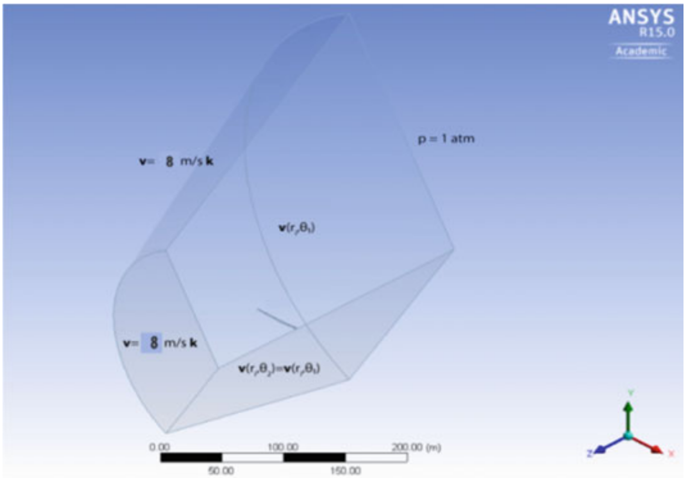

Fig. 6 Boundary conditions

0.05 m blade face sizing, is carried to find appropriate mesh face size at wind turbine blade surfaces. The boundary condition wind turbine CFD analysis is the wind speed 8.0 m/s, rotor rotational speed 15.0 rpm, and pitch angle 02.6° wind turbine blade.

The boundary conditions for this study are mentioned in Fig. 6, the velocity was given as 8 m/s normal to the domain face, and other faces are considered as pressure far fields.

2.3 *Solution Method*

In our work, $k - \omega$ Shear-Stress-Transport model is opted for turbulence modeling which will be more appropriate for the stimulation of far-field flows and modeling the boundary layer. This is a subsonic region problem of Mach number below 0.3 Mach, so incompressible 1.225 kg/m^2 constant density for air and constant viscosity 1.7894 $\times$ 10^{-5} kg/ms^{-1}. The incompressible RANS which is nothing but the Reynolds-Averaged Navier–Stokes equations are solved with the help of the coupled algorithm which is based on the pressure, which solves the pressure and as well as the momentum-based continuity equations in the form of closely coupled manner which significantly improves the rate of convergence (Ansys Fluent–16.0).

2.4 Convergence Criteria

To verify analysis of the CFD solution, imbalances of the residual values and net mass are examined. The solution is converged when these residual values are below than 10^{-4}, which is the common value used for residual convergence. The verification of the net mass imbalances confirms the convergence. The convergence of the net mass imbalance of an analysis is less than 0.1%.

3 Results and Discussions

Various advantages of wind turbines because of wind turbine vortex generators are discussed below.

3.1 Pressure Distributions

The pressure distributions on various airfoil sections of the wind turbine with and without vortex generators are shown Fig. 7. The low negative pressure is resulted in the rear blade surface due to the large negative pressure on the leading edges of the blade and the large positive pressure next to the leading edge of blade which causes stagnation points shifted to the suction surface because of reduced air velocity. Pressure sign reversed by pitching action and also results in faster moving airflow over the lower side of the blade lead to low suction on the pressure surface.

3.2 Velocity Contour

The velocity contour on various airfoil sections of the wind turbine with and without vortex generator are shown Fig. 8. The flow separation on airfoil sections without vortex generators can be visualized on the velocity contour. There is flow separation on one-third of the chord of the airfoil of the wind turbine. Because of vortex generator

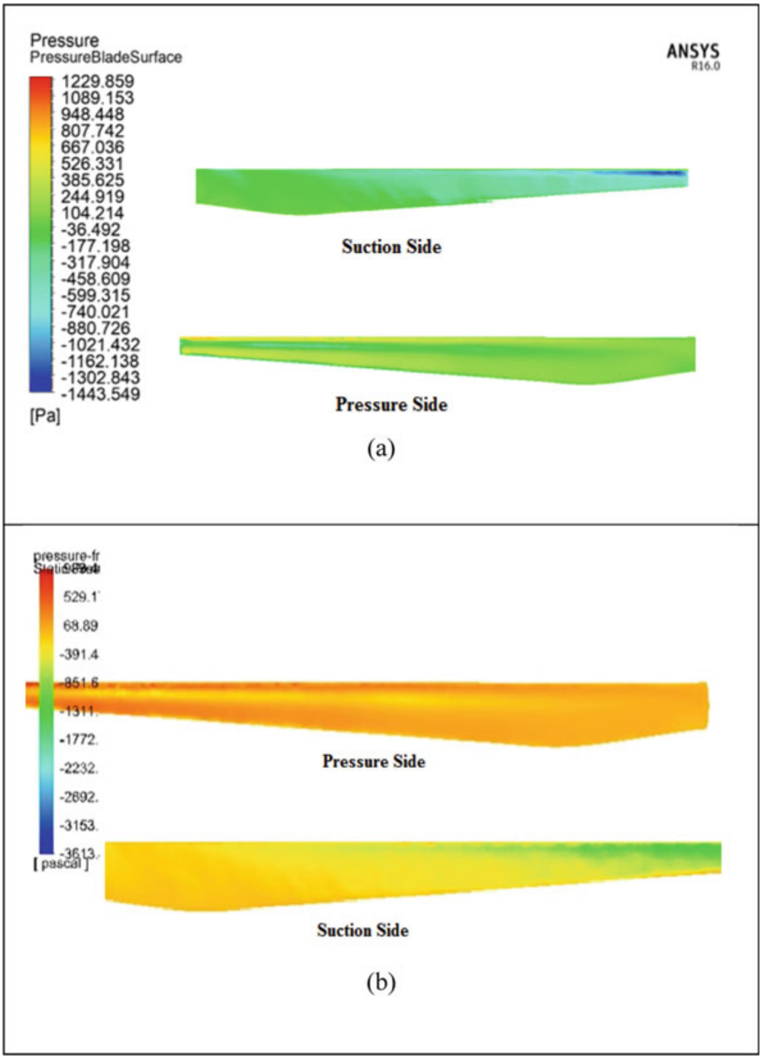

Fig. 7 Pressure distribution along blade **a** without VF **b** with VF

application on airfoils of turbine blade, there is stall delay and also stabilizes the flow over the blade surface. The above-discussed effects will result in an increase in performance of the wind turbine.

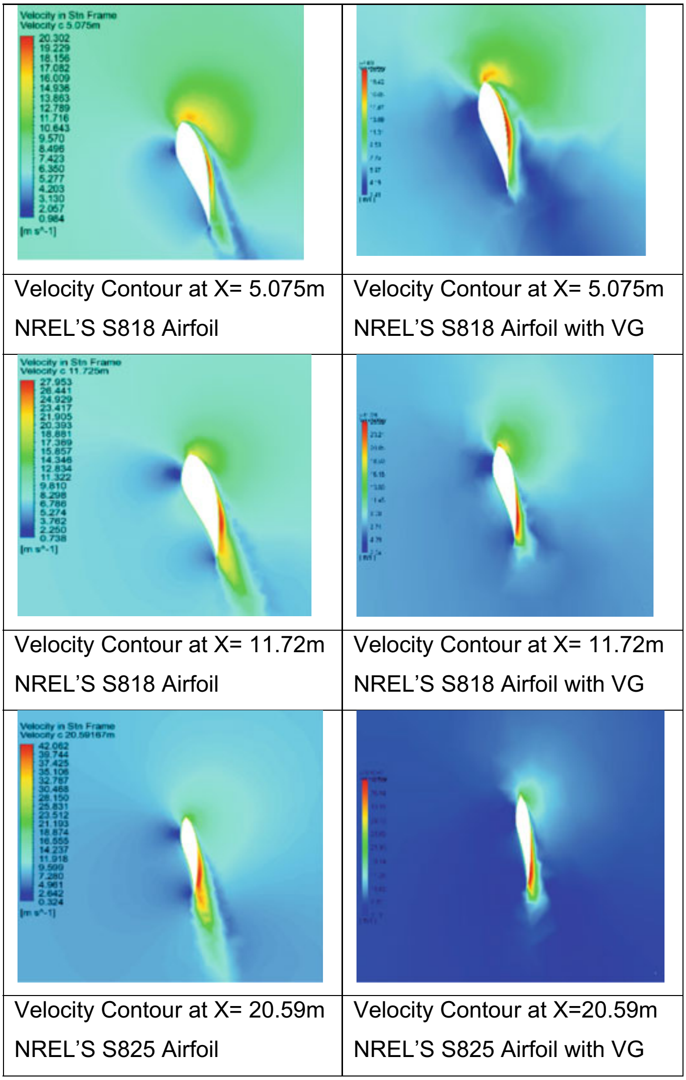

Fig. 8 Velocity distribution around airfoil cross section with and without VG

3.3 Velocity Vector

From the velocity vector, there is an increase in velocity found when the blade with VG along the span of blade. The variation of velocity along the blade was in accordance with the one-dimensional mathematical calculation of the wind turbine. Velocity vector is shown in Fig. 9.

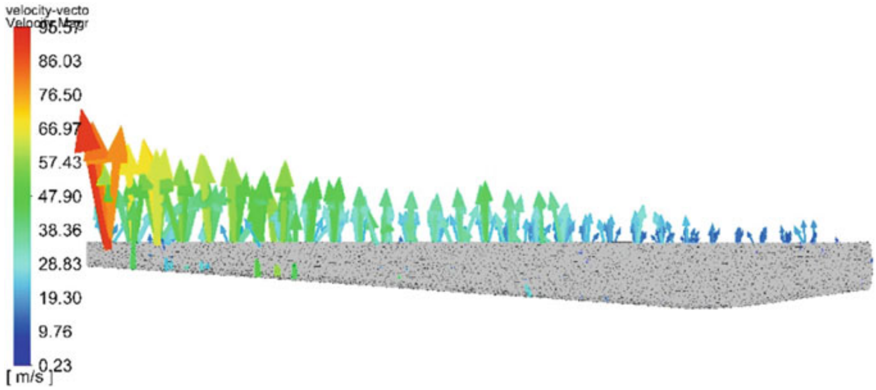

Fig. 9 Velocity vector on blade surface with vortex generator

4 Conclusion

In this study, the aerodynamic effects of the vortex generator in the wind turbine blade are visualized by using computational approach. The WindPACT 1.5-megawatt turbine is taken as a reference and has S818+, S825+, and S826+ airfoils, and vortex generators are placed along the length of blade. The CFD analysis is done for the wind speed 08 m/s, rotor rotational speed 015 rpm, and pitch angle 02.6°. For turbulence modeling, the $k - \omega$ SST model is used and various analyses were done to ensure mesh independency. The local airfoil's pressure and velocity are compared and discussed about the wind turbine blades in two different cases which consist of vortex generators and which does not have vortex generators. This study shows the results in flow stability and decrease in flow separation and stall of the wind turbine blade in which the vortex generators are placed along the length of the turbine. Because of this aerodynamic effect of vortex generator, the performance of turbine was increased.

References

1. Abbot IH, Von Doenhoff AE, Stivers LS (1945) Summary of airfoil data
2. Baker JP, Mayda EA, van Dam CP (2006) Experimental analysis of thick blunt trailing-edge wind turbine airfoils. J Sol Energy Eng 128:422. https://doi.org/10.1115/1.2346701
3. Barlow JB, Rae WH, Pope A (1999) Low-speed wind tunnel testing, 3rd edn. Wiley, New York
4. Griffin DA (1996) Investigation of vortex generators for augmentation of wind turbine power performance. National Renewable Energy Lab., Golden, CO
5. Johnson SJ, Berg DE (2008) Active load control techniques for wind turbines. Sandia National Laboratories
6. Khoshvaght-Aliabadi M, Sartipzadeh O, Alizadeh A (2015) An experimental study on vortex-generator insert with different arrangements of delta-winglets. Energy 82(C):629–639

7. Dykes KL, Rinker J (2018) WindPACT reference wind turbines. United States: N. p., 2018. Web. https://doi.org/10.2172/1432194
8. IRENA (2019) Renewable capacity statistics (2019) Report. International Renewable Energy Agency (IRENA)